Combustion and Flame 158 (2011) 172–178

Contents lists available at ScienceDirect

Combustion and Flame

journal homepage: www.elsevier.com/locate/combustflame

Auto-ignition of toluene-doped *n*-heptane and iso-octane/air mixtures: High-pressure shock-tube experiments and kinetics modeling

M. Hartmann [a,*], I. Gushterova [b], M. Fikri [a], C. Schulz [a], R. Schießl [b], U. Maas [b]

[a] Institute for Combustion and Gasdynamics (IVG), University of Duisburg-Essen, Duisburg, Germany
[b] Institute for Technical Thermodynamics (ITT), Karlsruhe Institute of Technology (KIT), Karlsruhe, Germany

ARTICLE INFO

Article history:
Received 31 March 2010
Received in revised form 29 July 2010
Accepted 16 August 2010
Available online 28 September 2010

Keywords:
Auto-ignition
Toluene
TRF
High-pressure shock tube
Chemical kinetics modeling

ABSTRACT

Toluene is often used as a fluorescent tracer for fuel concentration measurements, but without considering whether it affects the auto-ignition properties of the base fuel. We investigate the auto-ignition of pure toluene and its influence on the auto-ignition of *n*-heptane and iso-octane/air mixtures under engine-relevant conditions at typical tracer concentrations. Ignition delay times τ_{ign} were measured behind reflected shock waves in mixtures with air at $\varphi = 1.0$ and 0.5 at $p = 40$ bar, over a temperature range of $T = 700$–1200 K and compared to numerical results using two different mechanisms. Based on the models, information is derived about the relative influence of toluene on τ_{ign} on the base fuels as function of temperature. For typical toluene tracer concentrations $\leqslant 10\%$, the ignition delay time τ_{ign} changes by less than 10% in the relevant pressure and temperature range.

1. Introduction

In internal combustion (IC) engine research and development, detailed information about the mixture formation is crucial. Laser-induced fluorescence (LIF) methods are frequently applied to study the mixture formation [1] because they allow spatially and temporally resolved non-intrusive measurements. Commercial fuels often contain a complex mixture of fluorescing components, making it complicated to infer quantitative fuel concentrations from measured LIF signal intensities. Therefore, fluorescent tracers are often applied and added to otherwise non-fluorescing surrogate fuels [2]. Among these fluorescing tracers, toluene ($C_6H_5CH_3$) is widely used for visualizing the fuel distribution in IC engines via LIF [3]. This tracer is of particular interest for engine research, because it is present in many fuels as a major aromatic component. Thus, no "exotic" component needs to be introduced into the fuel. However, due to the lack of detailed information, in most cases fluorescent tracers are added without considering their effect on the ignition properties of the base fuel. Understanding the interaction between toluene and fuel chemistry in detail can in turn also help to develop improved fuels, by tailoring their composition so that they meet certain criteria (e.g., predictable auto-ignition properties).

Toluene auto-ignition has been subject of several experimental and numerical studies. Most of these studies (e.g. [4,5]) focus on the oxidation of toluene mixtures with oxygen that are highly diluted with inert gases, for low pressures and high temperatures in shock tubes. Sivaramakrishnan et al. [6] presented a detailed chemical kinetics model to predict the oxidation of toluene for temperatures with 1200 K < T_5 < 1500 K for a wide pressure range (25 bar < p_5 < 610 bar) and validated this model against experimental data obtained in a high-pressure single-pulse shock tube (p_5 and T_5 refer to the conditions behind the reflected shock wave). Only few numerical and experimental data for toluene oxidation with and without model fuels like *n*-heptane or iso-octane can be found in literature. Gauthier et al. [7] investigated *n*-heptane/air, surrogate gasoline fuels as well as a 10-component "research gasoline" (RD387). Davidson et al. [8] studied iso-octane/air and toluene/air combustion under engine-relevant conditions. Andrae et al. [9] used the experimental data of Herzler et al. [10] and Gauthier et al. [7] to develop a detailed kinetics mechanism describing the auto-ignition of toluene reference fuels (TRF). Mittal et al. [11] investigated the auto-ignition of pure toluene at elevated pressures in a rapid compression machine for 920 K < T < 1100 K and various oxygen concentrations. Among recent studies, Shen et al. [12] studied the ignition of toluene at high temperatures and at high pressures and compared the results with the prediction of the available models (Pitz [13], Andrae [9], Sakai [14]). The experimental results were also compared with the findings of Davidson et al. [8] and Mittal and Sung [11]. The comparison showed that the results of Davidson et al. at stoichiometric conditions exhibit an activation energy almost two times smaller than reported by Shen [12]. They attributed the disagreement to the occurrence of the

* Corresponding author. Fax: +49 2033793087.
E-mail address: michaela.hartmann@uni-due.de (M. Hartmann).

0010-2180/$ - see front matter © 2010 The Combustion Institute. Published by Elsevier Inc. All rights reserved.
doi:10.1016/j.combustflame.2010.08.005

pre-ignition in the Davidson's experiments [8] originating from contamination of their shock tube. A new study by Vasu et al. [15] refuted the finding of Shen et al. [12] by investigating the influence of the wall passivation (i.e. purging the shock tube with the respective gas mixture before evacuating and filling with the test gases), pollutant effects, and impurities resulting from inappropriate shock tube cleaning strategies on the measured ignition delay times of stoichiometric toluene/air mixtures for pressures near 50 bar and temperatures of 966–1211 K. They attributed the pre-ignition characteristics seen in the pressure profiles to the nature of the ignition regime in the different temperature ranges and found that the pre-ignition does not impact the accuracy of the ignition delay times. The determined activation energies of the ignition delay times show good agreement with the earlier data of Davidson et al. [8] and show differences to the RCM data of Mittal et al. [11].

For pure model fuels, ignition delay time measurements under engine-relevant conditions can be found, e.g. [7,8,16–18]. Experimental data of the auto-ignition of toluene-doped fuels, however, are still rare.

Few papers addressed the interaction of fluorescence tracers and fuels. A recent study by Westbrook and Sick investigated the stability of biacetyl relative to reference fuels based on kinetics models, however, without experimental validation [19].

In this paper we performed shock-tube measurements of ignition delay times to further validate the existing TRF mechanism based on our previous experimental results for low toluene concentration in *n*-heptane or iso-octane/air mixtures [20]. Numerical studies are then performed to assess the influence of toluene onto the ignition behavior of iso-octane and *n*-heptane. Furthermore, numerical simulations are employed to study the decomposition of toluene under in-cylinder conditions and its significance for the use of toluene as a representative for local fuel concentration or as an indicator for the time and the position of the onset of the heat release.

2. Experimental

Ignition delay times have been measured in a heatable high-pressure shock tube under engine-relevant conditions. The shock tube has a constant inner diameter of 90 mm. The driver section is 6.4 m long and the driven section has a length of 6.1 m. The two parts are separated by an aluminum diaphragm with typically 4 mm thickness. The maximum test time is extended up to 15 ms by driver gas tailoring [21]. Helium and Argon are mixed in-situ with two high-pressure mass flow controllers (Bronkhorst). Their composition is calculated using equations by Oertel [22] and Palmer and Knox [23]. To ensure complete evaporation of the liquid fuels, the test section of the shock tube and the gas manifold was heated to 350 K. Mixtures were prepared in the driven section. The fuel was injected directly into the evacuated driven section at $p < 2 \times 10^{-2}$ mbar. The injection septum is positioned almost in the middle of the driven section. After evaporation, which is determined from the observation of pressure, synthetic air (79.5% N_2, 20.5% O_2) was added manometrically to prepare the desired equivalence ratio. The mixtures settled for at least one hour to ensure homogeneous mixing. Earlier tests showed that with the fuel used here the measured ignition delay times did not depend on the mixing time as long as a minimum of 60 min is exceeded [17,18].

The incident shock speed is determined from three piezo-electric pressure transducers near the measurement section. The temperature and pressure behind the reflected shock wave were computed from the incident shock velocity, its attenuation and the initial conditions T_1 and the filling pressure p_1 using a one-dimensional shock tube code (Chemkin [24]). The principle of the determination of τ_{ign} from the CH* and pressure signals is shown in Fig. 1 for an example signal trace for stoichiometric toluene/iso-octane (10/90% per volume) ignition in air at $p = 42.0$ bar and $T = 821$ K. The steepest increase in CH* chemiluminescence intensity as well as the pressure rise is observed at 4.6 ms after arrival of the reflected shock wave as indicated by the dashed tangent at the CH* signal. The ignition delay time is defined as the delay between the arrival of the reflected shock wave and the intersection of the steepest tangent with zero chemiluminescence signal.

3. Chemical kinetics model

For the simulation studies, the toluene reference fuel (TRF) mechanism of Andrae et al. [25] was used, containing 633 reactions of 137 species. This mechanism has been shown by its authors to well predict ignition delays for a range of engine-relevant pressures and temperatures. Because the mechanism is only semi-detailed in nature (it is based on skeletal mechanisms for iso-octane and *n*-heptane), additional numerical studies were also performed using the Lawrence Livermore PRF (primary reference fuel) mechanism [26], augmented by a toluene submechanism of Andrae et al. [9]. This was done to ascertain whether tracer-relevant results obtained with the semi-detailed mechanisms were also found when the more detailed scheme was used in the simulations.

4. Numerical simulations

Various numerical simulations were performed for comparing predicted ignition delay times with the shock-tube measurements. The calculations were based on a homogeneous reactor model with semi-detailed chemistry according to the TRF mechanism [25]. An adiabatic constant volume model was used in these simulations; the governing equations describing this model are given in [27]. The simulations delivered the detailed temporal development of temperature, pressure and species mole fractions resulting from chemical reactions. Ignition delay times were determined from the CO_2 mole fraction vs. time curve by forming the tangent at the location of the steepest increase and then determining the intersection of this tangent with the time axis (x-axis). Alternatively, the ignition criterion was based on a similar analysis of CO and OH, which, however, caused no notable difference in the resulting value for the ignition delay.

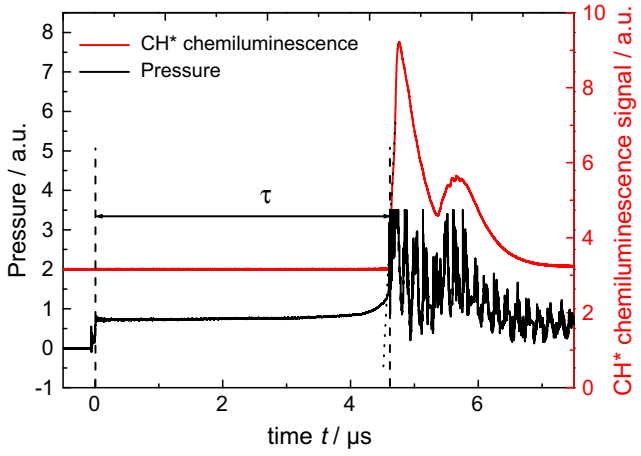

Fig. 1. Typical pressure and CH* chemiluminescence profile for a stoichiometric iso-octane/toluene (90/10 vol.%)/air mixture with $T = 821$ K and $p = 42.0$ bar. Data traces after the initial rise after ignition do not have a quantitative meaning.

Several simulations were performed in a parametric study with initial conditions set according to the shock-tube experiments, covering a range of fuel compositions, temperatures, and equivalence ratios. The fuel compositions studied included pure iso-octane, pure *n*-heptane, toluene, and mixtures of iso-octane and *n*-heptane with toluene. This allowed constructing global ignition delay time maps which exhibit the influence of toluene on the ignition behavior of the reference fuels.

5. Results and discussions

5.1. Ignition delay time

Ignition delay times were determined for different fuel (*n*-heptane and iso-octane)/air mixtures (φ = 1.0 and 0.5) with 0, 10, and 40 vol.% toluene, respectively for p = 40 ± 2 bar over a wide temperature range of 700–1200 K. Table 1 summarizes the results of the ignition delay times for all fuels and reaction conditions investigated in this study.

Figure 2 shows the comparison of measured and simulated ignition delay times for iso-octane with and without 10 vol.% toluene for p = 40 bar and φ = 1.0 and 0.5, respectively. In this Arrhenius diagram, τ_{ign} is plotted logarithmically over the inverse post-reflected shock temperature T_5. Both, experiment and simulation show longer ignition delay times for lean mixtures, as expected. For all measurements and simulations a comparable shape of the curves is found. The simulations for toluene-doped iso-octane with φ = 1.0 show no difference in the ignition delay times compared to the case with pure iso-octane. The difference in τ_{ign} between toluene-doped and pure fuels is more pronounced in the experimental results especially in the low-temperature range. However, the influence of the toluene concentration on the ignition delay time is small.

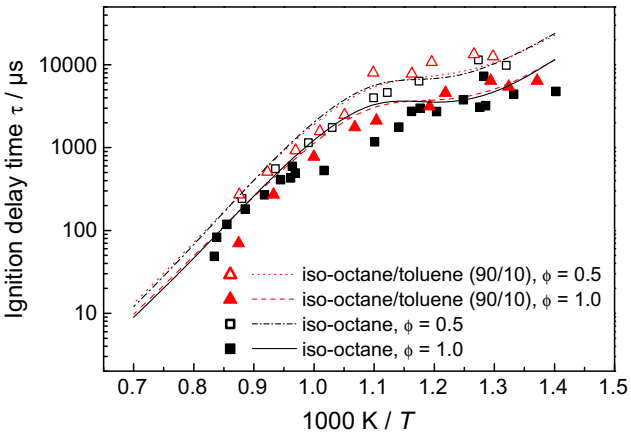

Fig. 2. Comparison of measured and simulated τ_{ign} for toluene/iso-octane (10/90 vol.%) and iso-octane/air mixtures for p = 40 bar and φ = 1.0 and 0.5. Symbols: experiments, lines: simulations with semi-detailed mechanism [25].

Table 1
Ignition delay times of the fuels and conditions investigated in this work.

T/K	p/bar	$t/\mu s$	T/K	p/bar	$t/\mu s$	T/K	p/bar	t/μs	T/K	p/bar	$t/\mu s$
Toluene/n-heptane			*n-Heptane in air, φ = 1.0*			*Toluene in air, φ = 0=0.5*			*Toluene/n-heptane*		
(10/90 vol%) in air, φ = 1.0			692	40.9	3148	942	40.4	8815	*(40/60 vol%) in air r, φ = 0.5*		
713	38	2487	695	41.4	2696	967	39	5144	858	41.5	1615
717	39.3	2075	705	32_075	1975	1029	40.5	1998	919	41.5	1623
731	44.4	1223	735	40.2	1008	1069	39.9	1300	1003	40.7	975
759	41.4	894	767	40.9	680	1115	39.6	783	*n-heptane in air, φ = 0.5*		
763	38.3	948	769	43	632	1140	36.5	545	739	42.5	1564
770	40.5	778	823	41	376	*Toluene/iso-octane*			812	42.6	431
799	38.2	611	836	38	386	*(10/90 vol%) in air, φ = 1.0*			826	38.2	520
813	42.5	533	841	43	311	729	41.2	6421	853	38.5	551
835	38.9	537	880	42.9	320	755	40.3	5443	860	36.4	559
850	37.7	530	882	42.6	334	773	40	6416	885	42.4	427
871	42.7	434	8214	43.4	286	821	42	4604	970	43.2	601
882	40.6	433	933	42.4	408	839	37.2	3152	1033	41.4	505
906	40.1	604	937	42.3	488	906	41.7	2125	1165	45.1	110
920	39.2	685	970	42	483	937	40.1	1762	1247	44.3	20
920	39.7	558	984	43.3	432	1000	40.7	779	1275	46.7	10
953	40.4	603	990	39.2	394	1072	41.8	271	*Toluene/iso-octane*		
957	39.1	670	1030	47.2	264	1143	43.7	70	*(10/90 vol%)in ai r, φ = 0.5*		
1007	43.9	504	1032	42.8	319	*Iso-octane in air, φ = 1.0*			771	41.8	12592
1022	41.3	299	1040	43.6	297	713	38.9	4754	790	39.6	13420
1038	41.3	372	1072	47	218	751	39.5	4396	836	41	10789
1041	37.3	316	1246	47.5	14	778	43.2	3202	860	40.6	7790
1061	39.9	290	1249	47.6	22	780	41.2	7272	910	41.1	8051
1174	47.7	66	1264	49.1	11	784	41.2	3075	952	40.9	2489
1181	47.8	52	*Toluene/n-heptane*			801	40.6	3787	990	40.2	1573
Toluene/n-heptane			*(10/90 vol%) in air, φ = 0.5*			831	40.9	2725	1031	39.6	925
(40/60 vol.%) in air, φ = 1.0			709	40.8	2847	850	40	2979	1084	40	509
846	40	711	731	44.4	1223	860	41.2	2740	1142	40.8	271
898	39.5	684	755	39.7	1441	876	43.1	1763	*Iso-octane in air φ = 0.5*		
1015	41.2	574	759	41.2574	894	908	42.8	1176	758	40	9853
Toluene in air, φ = 1.0			790	39	1188	984	43	530	785	39	11485
859	42.3	4911	835	39.4	768	1032	42.5	492	851	43.2	6346
882	41.6	3214	848	40.9	750	1037	43	593	891	42.5	4629
911	41.7	3375	889	39.9	704	1040	41	430	910	39.8	4004
954	43.4	2276	930	38.7	682	1059	42.7	410	971	40.4	1748
996	44	1529	999	40.3	848	1129	42	181	1009	39.1	1143
1034	42.9	1256	12561	39.9	290	1169	42	119	1068	39.5	555
1100	40.2	639	1082	40.7	291	1193	43.2	83	1136	40.3	242
1149	39	342	1185	42.4	43	1199	40.9	49			

For the experiments at $\varphi = 0.5$ with and without toluene the difference in ignition delay times is more pronounced especially in the low-temperature range. The experiments show toluene to act as ignition inhibitor. The simulation, however, cannot resolve this effect. When comparing the lean and the stoichiometric toluene-doped iso-octane, the ignition delay times characteristics of the mixture follow the overall ignition chemistry of the main fuel, and the toluene when used as additive does not affect globally the kinetics of the main fuel, here iso-octane. The simulation reflects also the same result.

Simulations and experiments show the same trend for the ignition delay times in the Arrhenius diagrams. The simulations overpredict the measured τ_{ign} systematically. The effect increases with decreasing temperature. For high temperatures ($T > 1000$ K), both results are in good agreement. However, Fig. 2 shows that when comparing the simulated ignition delay to the measured for the iso-octane/toluene mixture at $\varphi = 0.5$, the model underpredicts the experiments at lower temperatures.

Figure 3 shows the comparison of measured and simulated τ_{ign} for *n*-heptane with and without 10, 40, and 100 vol.% toluene for $p = 40$ bar and $\varphi = 1.0$ (upper part) and 0.5 (lower part of the figure). The absolute values of τ_{ign} are shorter than for iso-octane, as expected. The pronounced S-shaped curve, indicating a negative temperature coefficient (NTC) regime due to the main component *n*-heptane is observed for 10 vol.% toluene doping in simulations and measurements as well. The ignition delay time for the lean mixtures is longer than for stoichiometric mixtures and the influence of toluene on τ_{ign} is small for the mixture with $\varphi = 1.0$. The lean mixture is slightly influenced by the 10 vol.% toluene doping.

With increasing toluene concentration, a decrease in the NTC behavior is observed. For the stoichiometric mixture, the ignition delay times with 40% toluene is increased up to 30% at 850 K. The lean mixture with $\varphi = 0.5$, however, shows a more pronounced increase in τ_{ign} due to the longer absolute delay times, but the relative increase is the same with a factor of 1.3 at the same temperature. Because the purpose of the work was to investigate the applicability limit of toluene as tracer, and the typical tracer concentrations usually do not exceed 20%, only a few experimental points have been investigated for 40 vol.% toluene in *n*-heptane. These measurements were used to demonstrate the performance of the semi-detailed mechanism in a wider concentration range [25]. Pure toluene/air mixtures show a linear behavior in the Arrhenius diagram for both fuel/air ratios.

The differences between simulated and measured τ_{ign} decrease with increasing toluene concentration, and for $\varphi = 0.5$, they are negligible. For $\varphi = 1.0$ differences between measurements and simulations are still observed even for pure toluene/air combustion with $T < 1000$ K. In principle, however, it is possible to describe the auto-ignition of toluene and mixtures with high toluene doping levels quite well using the TRF mechanism by Andrae et al. [25]. Both, simulations and measurements show that the NTC behavior disappears with increasing toluene concentration.

The literature does not provide much data of the auto-ignition of toluene in this temperature and pressure region. Davidson et al. [8] investigated the ignition delay times of toluene/air mixtures for $\varphi = 1.0$ and 0.5 at 17 bar and 50 bar and $T_5 > 980$ K. They found linear behavior of the τ_{ign} in the Arrhenius diagram indicating that there is no change in the combustion chemistry of toluene within that temperature range. The rapid compression machine (RCM) experiments performed by Mittal et al. give ignition delay data for 25 and 45 bar for various equivalence ratios and temperatures between 920 and 1100 K. Recently, Shen et al. investigated the toluene oxidation in the temperature range of 1021–1400 K and pressures up to 61 bar [12]. Their data does not show any decrease of activation energy contrary to the results of Davidson. To our knowledge, our measurements of pure toluene in stoichiometric mixtures with air are the first performed under engine-relevant conditions and at such low-temperatures in a shock tube. A comparison of the literature data with the present results is shown in Fig. 4. The ignition delay times of Davidson et al. are scaled to 40 bar (original data is taken from the 50 bar pressure range only to minimize scaling errors) using the pressure dependence evaluated by the authors with $\tau(\varphi = 1.0) = 2.9 \times 10^{-6}\ (p/\text{atm})^{-0.93} \exp(9410\ \text{K}/T)$ s and $\tau(\varphi = 0.5) = 5.4 \times 10^{-9}\ (p/\text{atm})^{-0.50} \exp(15{,}455\ \text{K}/T)$ s. Mittal's data have been scaled (only the original 45 bar experiments) linearly in pressure according to the results Vasu et al. present for their investigations for the stoichiometric toluene/air condition at ~50 bar [15]. Their data were linearly scaled in pressure to 40 bar to ensure the comparability to the present study. Linear regression of our data fits to the correlated ignition delay times from our measurements:

$$\varphi = 1.0 : \tau = (3.98 \pm 0.78) \times 10^{-7} \exp(8157 \pm 761\ \text{K}/T)\ \text{s}$$
$$\varphi = 0.5 : \tau = (1.53 \pm 0.46) \times 10^{-9} \exp(14{,}584 \pm 473\ \text{K}/T)\ \text{s} \quad (1)$$

Like Davidson et al. we observe a strong dependence of τ on φ. The activation energies, are comparable to those found by Davidson et al., even though for the stoichiometric mixture the present activation energy is smaller. The pressure dependence has not been investigated in the present work, as all experiments were conducted for 40 bar behind reflected shock waves. Shen et al. also

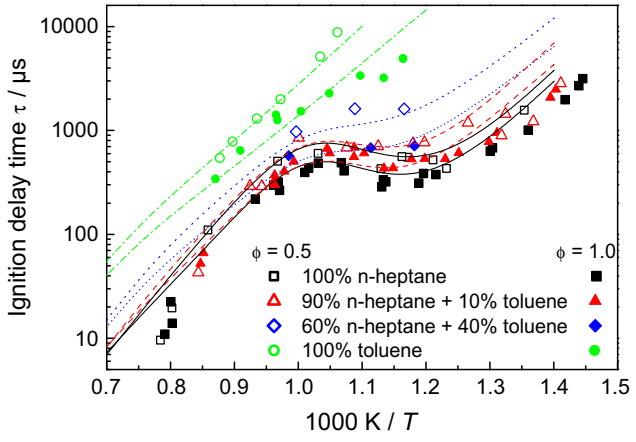

Fig. 3. Comparison of measured and simulated τ_{ign} for toluene/*n*-heptane (10/90 and 40/60 vol.%) and *n*-heptane/air mixtures for $p = 40$ bar and $\varphi = 1.0$ and 0.5 respectively.

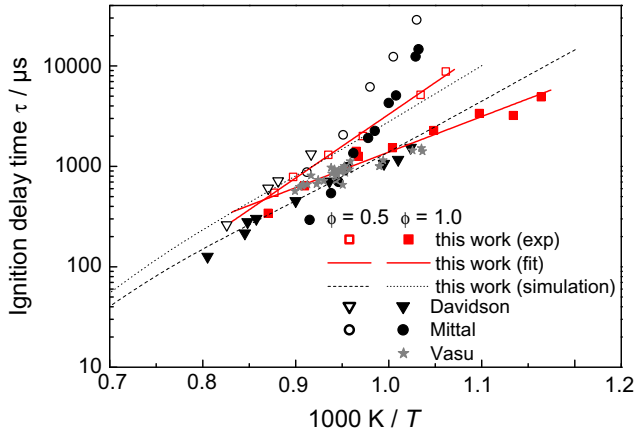

Fig. 4. Ignition delay times of toluene/air mixtures for $\varphi = 1.0$ (filled symbols) and 0.5 (open symbols) compared to shock-tube experiments by Davidson et al. [8] and Vasu et al. [15], and RCM experiments by Mittal et al. [11]. The simulations are based on the semi-detailed mechanism [25].

derived correlations from regression analysis for the ignition delay times at $\varphi = 1.0$, 0.5 and 0.25 [12]. The activation energy for $\varphi = 1.0$ was found to be 15,640 K^{-1} and also in good agreement with our results, for the lean mixture with $\varphi = 0.5$ their activation energy is with 15,330 K^{-1} a factor of two larger compared to Davidson's and our result. Figure 4 also shows the ignition delay times that are computed using the presented Arrhenius equations. The ignition delay times observed in the RCM differ significantly from those that come from shock-tube experiments. The difference in shock tube and RCM data has been subject of many other studies, e.g. [11,12,28–30] and the direct comparison of both sorts of data is known to be nontrivial, as shock tubes and RCM operate in different ways. The steeper slope in the Arrhenius diagram indicates a higher activation energy compared to the shock-tube results. The data of Davidson et al. shows slightly longer ignition delay times for $\varphi = 0.5$, but qualitatively the results are in good agreement with the preset study. The results of Vasu et al. for the stoichiometric combustion agree well with our data and the data by Davidson et al. However, until now no shock tube data for toluene ignition are available at lower temperature.

5.2. Influence of toluene on auto-ignition characteristics

To gain a more complete picture of the influence of toluene on the auto-ignition behavior of iso-octane/*n*-heptane mixtures, simulation results were studied for a number of toluene doping levels in iso-octane and *n*-heptane. The results for toluene in *n*-heptane are displayed in Fig. 5, while results for toluene in iso-octane are shown in Fig. 6 as contour-plots of the logarithm of ignition delay time. Both the results of Figs. 5 and 6 (just like the results from Figs. 7 and 8) were obtained using the semi-detailed TRF mechanism, by performing ignition delay time computations on 16×14 equidistant grid points in the diagram, and then plotting contour-lines through the resulting ignition delay time field. Predictions on the influence of toluene on ignition delay times obtained by the detailed (Lawrence Livermore PRF mechanism [26] augmented by a toluene submechanism [9]) and the semi-detailed TRF [25] mechanisms will be compared below.

Figure 5 shows that the characteristic NTC behavior of *n*-heptane disappears for higher toluene concentrations. For 40 vol.% toluene and above, the NTC behavior has almost disappeared in the simulations. This is in agreement with the measurements (see Fig. 3). For iso-octane (Fig. 6) as the main component, the ignition delay time does not show a strong dependence on the toluene concentration for temperatures between 900 and 1100 K, as seen by the nearly horizontal iso-lines of ignition delay time in this region. In the low-temperature region, τ_{ign} increases significantly with increasing toluene concentrations.

The relative effect of toluene addition on τ_{ign} of iso-octane and *n*-heptane is additionally illustrated by maps of the ratio

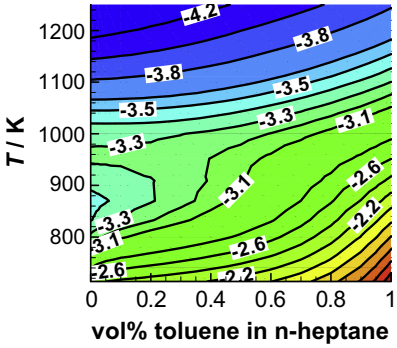

Fig. 5. Contour diagram of $\log_{10}(\tau_{ign}/s)$ as a function of temperature and toluene concentration in *n*-heptane, $\varphi = 1$, $p = 40$ bar. The contour labels give $\log_{10}(\tau_{ign}/s)$.

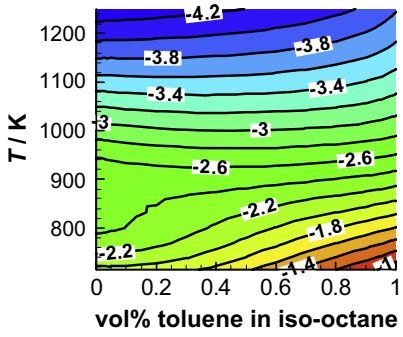

Fig. 6. Contour diagram of $\log_{10}(\tau_{ign}/s)$ as a function of temperature and toluene concentration in iso-octane, $\varphi = 1$, $p = 40$ bar (computed). The contour labels give $\log_{10}(\tau_{ign}/s)$.

τ_{ign}(fuel + tracer)/τ_{ign}(pure fuel). If this ratio is larger or smaller than unity, toluene has a decelerating or accelerating effect on the ignition, respectively. In the following the diagrams resulting from the detailed and semi-detailed mechanism are shown for both fuels to compare the predictability of both mechanisms.

Figure 7 shows a map of τ_{ign}(*n*-heptane + toluene)/τ_{ign}(*n*-heptane) as a function of temperature and toluene concentration in *n*-heptane. Diagram a) shows the result for the detailed mechanism, and diagram b) shows the result for the semi-detailed mechanism. Both mechanisms deliver a qualitatively similar behavior; importantly, both predict that for toluene levels below 10% (as typically used in tracer-LIF experiments), the alteration of ignition-delay time is less than 10%.

For toluene concentration below about 20%, its influence on the ignition delay is very small. The influence is stronger near 850 K than both at 1000 K and 750 K. The detailed and semi-detailed mechanism show very similar results, with the semi-detailed mechanism predicting a slightly stronger influence of toluene on the ignition delay at higher temperatures.

The global ignition behavior of toluene/iso-octane mixtures (derived from simulations) is shown in Fig. 8. Again, the ratio τ_{ign}(iso-octane + toluene)/τ_{ign}(iso-octane) is shown as a contour plot for various toluene concentrations and for a range of temperatures with 750 K < T < 1250 K. Again, despite their qualitatively different behavior, both mechanisms agree that for toluene concentrations below 10%, the influence of toluene on τ_{ign} is small, with ignition delays of mixtures deviating by less than 10% from those of pure iso-octane. The semi-detailed mechanism predicts a slight accelerating effect of toluene on iso-octane in the temperature range between about 900 K and 1100 K, while the detailed mechanism predicts a weak decelerating effect in this temperature region. However, for both mechanisms, the magnitude of the influence is very small. Also, both mechanisms agree that for T < 900 K, and T > 1100 K toluene has a decelerating effect on the ignition delay. The strength of this effect strongly depends on temperature.

The overall shape of the function τ_{ign}(fuel + tracer)/τ_{ign}(pure fuel) shows that both for iso-octane and *n*-heptane fuel the dependence of the ignition delay on the toluene concentration is highly nonlinear and also strongly temperature dependent. Especially, the ignition delay for a fuel/toluene mixture can in general not be determined by simply interpolating between ignition delays of pure fuel and pure toluene.

Based on the comparison of simulations and experiments, the TRF mechanism has been confirmed to realistically predict the ignition delays of iso-octane, *n*-heptane, and toluene, and also the influence of toluene on the ignition behavior of iso-octane and *n*-heptane within the investigated temperature, pressure, and equivalence ratio range. Based on the mechanism, therefore, a qualitative view of the ignition delay of TRF fuels (iso-octane/

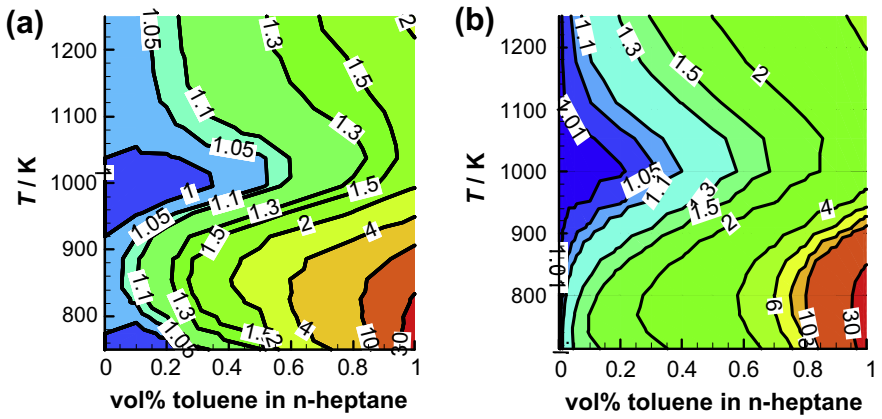

Fig. 7. Global map of the influence of toluene on the ignition delay of *n*-heptane for $p = 40$ bar, $\varphi = 1.0$ (simulation). The contours give the ratio τ_{ign}/τ_{ign} (pure fuel): (a) computed with the detailed TRF mechanism ([26] combined with [9] and (b) computed with the new TRF mechanism [25].

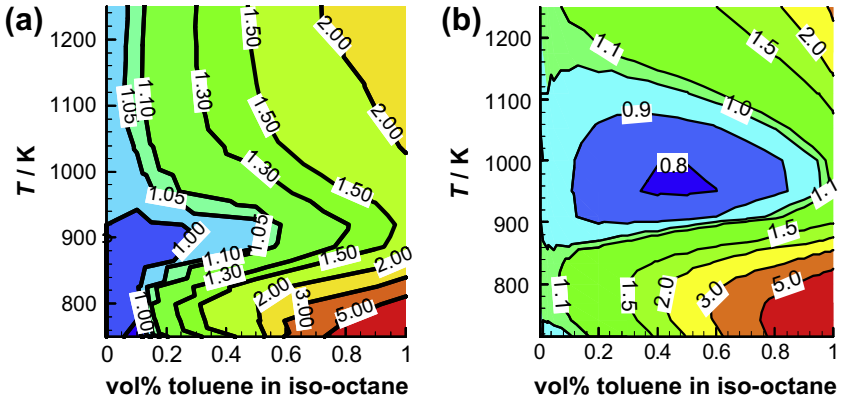

Fig. 8. Global map of the influence of toluene on the ignition delay of iso-octane for $p = 40$ bar, $\varphi = 1.0$ (simulation). The contours give the ratio τ_{ign}/τ(pure fuel): (a) computed with the detailed TRF mechanism ([26] combined with [9]) and (b) computed with the new TRF mechanism [25]).

n-heptane/toluene mixtures) can be computed. Such a view is provided in Fig. 9, which shows ternary diagrams of ignition delay times vs. relative amounts (mol%) of the three components. Along each side of the triangle, one of the three components is not contained in the mixture (as indicated), while the relative amounts of the other two components are varied between 0% and 100%. The two diagrams correspond to two temperatures (1000 K and 700 K), at a pressure of 40 bar and $\varphi = 1$. They were computed using the semi-detailed mechanism, by performing ignition delay time simulations at in total 55 operating conditions.

At 1000 K, 40 bar, and low *n*-heptane concentration, the mechanism predicts iso-lines of ignition delay that are nearly parallel to the 0% *n*-heptane line, which represents fuels with only toluene and iso-octane. Adding toluene to iso-octane has only little effect on the ignition delay, with a non-monotonic dependence of τ_{ign} on the amount of toluene in iso-octane. Pure iso-octane and toluene nearly have the same ignition delay at the conditions considered here. In contrast, addition of toluene to *n*-heptane has a clear retarding effect on the ignition delay. Iso-octane and toluene doping to *n*-heptane nearly have the same effect, increasing the ignition delay by roughly the same amounts. The diagram therefore appears nearly symmetric around its vertical axis.

At 700 K, and low *n*-heptane content, addition of toluene to iso-octane retards ignition from about 15 ms (100% iso-octane) to more than 80 ms (100% toluene). This retarding influence of toluene on iso-octane is very weak at low toluene levels, as seen by the fact that the 15 ms iso-line runs nearly parallel to the 0% *n*-heptane baseline near the lower right corner. Here, the ignition retardation of toluene mixed to *n*-heptane is much larger than the corresponding retardation of iso-octane ignition.

The ternary diagrams for the different temperatures show a variation in their overall appearance; at 1000 K, toluene and iso-octane nearly seem to have the same ignition retarding effect when mixed to *n*-heptane. At 700 K, in contrast, toluene is a stronger ignition retarder than iso-octane.

6. Conclusions

Ignition delay times for toluene/iso-octane (10/90% by volume) and toluene/*n*-heptane mixtures (10/90 and 40/60% by volume) have been determined in a high-pressure shock tube under engine-relevant conditions ($p = 40$ bar) for equivalence ratios $\varphi = 0.5$ and 1.0 over a wide temperature range with $700\ \text{K} < T < 1200\ \text{K}$. The results were compared to ignition delay times of the pure iso-octane and *n*-heptane fuels and to pure toluene/air mixtures under identical conditions.

The detailed Lawrence Livermore PRF mechanism [26], augmented by a toluene submechanism by Andrae et al. [9], was used in this study, as well as a more recently developed semi-detailed TRF mechanism [25]. A comparison of simulated and measured ignition delay times shows good agreement, although the

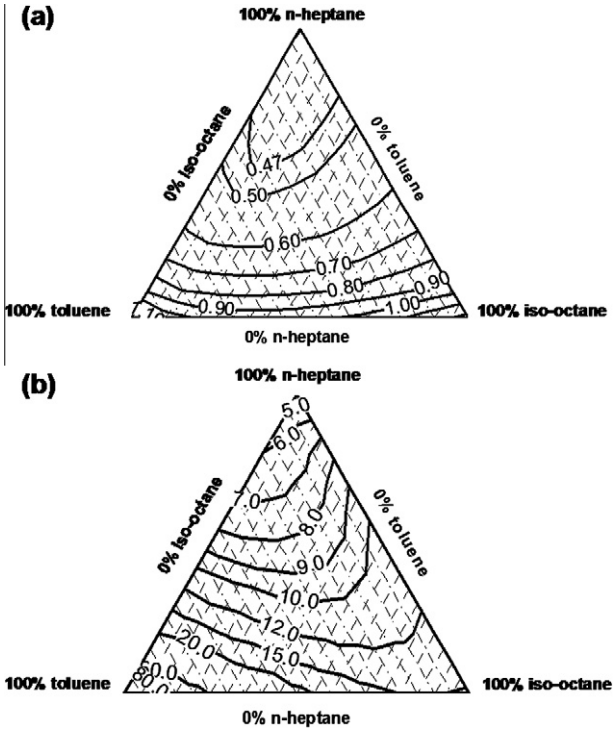

Fig. 9. Computed ignition delay times of iso-octane/*n*-heptane/toluene mixtures for $p = 40$ bar, $\varphi = 1$, (a) $T = 1000$ K, (b) $T = 700$ K under adiabatic, constant volume conditions (ternary diagram). The contour labels give the ignition delay time in ms.

simulations based on the detailed TRF mechanism systematically slightly overpredict the measured τ_{ign}. The new mechanism shows better agreement with the ignition delay times we measured in this study. Simulation and experiments indicate longer ignition delay for lean mixtures of fuel and toluene. This effect is more pronounced for iso-octane than for *n*-heptane due to the longer ignition delay of the base fuel (e.g. iso-octane). It was found that the kinetics of the toluene does not affect the ignition of the parent fuel when the former is used in sufficiently small concentration as a tracer. Specifically, for small toluene concentrations (<10% by volume) simulations and experiments at 40 bar do not show a significant effect of toluene on the auto-ignition of iso-octane and *n*-heptane.

Global maps of ignition delay times have been computed for the mixtures in order to reduce the number of required measurements for validating and/or improving the mechanism by revealing the temperatures and pressures where experimental effort should be spent. Simulations for a wider range of toluene concentrations show a stronger influence of toluene at doping levels >50% at lower temperatures ($T < 900$ K), while at temperatures of 900–1100 K, the effect is much weaker. In iso-octane, toluene shows a strong retarding effect on ignition delay for temperatures below about 900 K, while between about 900 and 1100 K, the effect of toluene on ignition delay is weaker. The detailed mechanism and the semi-detailed mechanism predict a qualitatively similar effect of toluene addition to iso-octane and *n*-heptane, even though the absolute values of ignition delays differ slightly. Ignition delay diagrams for iso-octane/*n*-heptane/toluene mixtures have been computed, which show that the qualitative influence of toluene on primary reference fuels strongly depends on temperature.

As a result found in simulations and already confirmed by experiments, toluene does not alter the ignition delay by more than ~10% compared to pure iso-octane or pure *n*-heptane if the amount of toluene in the mixture does not exceed 10% by volume. As comparison, the deviation of 10% in ignition delay times would roughly reflect a change of 2% in the octane number assuming iso-octane as test fuel.

For applications where toluene is used as a tracer for laser-induced fluorescence experiments (e.g. in engines), this means that at these low concentration levels, no significant alteration of the auto-ignition behavior of *n*-heptane or iso-octane fuel is expected near 40 bar.

Acknowledgments

The authors thank Natascha Schlösser for support in conducting the high-pressure shock-tube experiments. Financial support by the German Research Foundation is gratefully acknowledged. The authors are grateful to H.J. Curran, W.J. Pitz, and C.K. Westbrook, as well as J. Andrae, P. Björnbom, R. Cracknell and G. Kalghatgi, for making their PRF/TRF reaction mechanisms accessible to the combustion community.

References

[1] M.C. Drake, D.C. Haworth, Proc. Combust. Inst. 31 (2007) 99–124.
[2] C. Schulz, V. Sick, Progr. Energy Combust. Sci. 31 (2005) 75–121.
[3] W. Koban, C. Schulz, SAE Techn. Paper Series 2005-01-2091, 2005.
[4] A. Burcat, R.C. Farmer, R.L. Espinoza, R.A. Matula, Combust. Flame 36 (1979) 313–316.
[5] M.A. Oehlschlaeger, D.F. Davidson, R.K. Hanson, Combust. Flame 147 (2006) 195–208.
[6] R. Sivaramakrishnan, R.S. Tranter, K. Brezinsky, Proc. Combust. Inst. 30 (2005) 1165–1173.
[7] B.M. Gauthier, D.F. Davidson, R.K. Hanson, Combust. Flame 139 (2004) 300–311.
[8] D.F. Davidson, B.M. Gauthier, R.K. Hanson, Proc. Combust. Inst. 30 (2005) 1175–1182.
[9] J.C.G. Andrae, P. Björnbom, R.F. Cracknell, G.T. Kalghatgi, Combust. Flame 149 (2007) 2–24.
[10] J. Herzler, M. Fikri, K. Hitzbleck, R. Starke, C. Schulz, P. Roth, G.T. Kalghatgi, Combust. Flame 149 (2007) 25–31.
[11] G. Mittal, C.J. Sung, Combust. Flame 150 (2007) 355–368.
[12] H.-P.S. Shen, J. Vandover, M.A. Oehlschlaeger, Proc. Combust. Inst. 32 (2009) 165–172.
[13] W. J. Pitz, R. Seiser, J. W. Bozzelli, Second Joint Meeting of the U.S. Sections for the Combustion Institute, 2001.
[14] Y. Sakai, H. Ozawa, T. Ogura, A. Miyoshi, M. Koshi, W. J. Pitz, SAE Technical Paper Series 2007-01-4104, 2007.
[15] S. Vasu, D.F. Davidson, R.K. Hanson, J. Propulsion Power 26 (2010) 776–783.
[16] K. Fieweger, R. Blumenthal, G. Adomeit, Combust. Flame 109 (1997) 599–619.
[17] M. Hartmann, M. Fikri, R. Starke, C. Schulz, Proc. European Combustion Meeting, Chania, Greece, 2007.
[18] M. Hartmann, K. Tian, C. Hofrath, M. Fikri, A. Schubert, R. Schießl, R. Starke, B. Atakan, C. Schulz, U. Maas, F. Kleine Jäger, K. Kühling, Proc. Combust. Inst. 32 (2009) 197–204.
[19] V. Sick, C.K. Westbrook, Proc. Combust. Inst. 32 (2009) 913–920.
[20] M. Hartmann, I. Gushterova, R. Schießl, U. Maas, C. Schulz, Proc. European Combustion Meeting, Vienna, Austria, 2009.
[21] J. Herzler, L. Jerig, P. Roth, Combust. Sci. Technol. 176 (2004) 1627–1637.
[22] H. Oertel, Stoßrohre, Springer Verlag, Wien, New York, 1996.
[23] H.B. Palmer, B.E. Knox, ARS J. 31 (1961) 826–828.
[24] R.J. Kee, F.M. Rupley, J.A. Miller, M.E. Coltrin, J.F. Grcar, E. Meeks, H.K. Moffat, A.E. Lutz; G. Dixon-Lewis, M.D. Smooke, J. Warnatz, G.H. Evans, R.S. Larson, R.E. Mitchell, L.R. Petzold, W.C. Reynolds, M. Carcotsios, W.E. Stewart, P. Glarborg, C. Wang, O. Adigun, CHEMKIN Collection, Release 3.6, Reaction Design, Inc., San Diego (CA), 2000.
[25] J.C.G. Andrae, T. Brinck, G.T. Kalghatgi, Combust. Flame 155 (2008) 696–712.
[26] H.J. Curran, P. Gaffuri, W.J. Pitz, C.K. Westbrook, Combust. Flame 129 (2002) 253–280.
[27] U. Maas, J. Warnatz, Combust. Flame 74 (1988) 53–69.
[28] D.F. Davidson, R.K. Hanson, Int. J. Chem. Kinet. 36 (2004) 510–523.
[29] J. Würmel, E.J. Silke, H.J. Curran, M.S. Conaire, J.M. Simmie, Combust. Flame 151 (2007) 289–302.
[30] C. Mohamed, Combust. Flame 112 (1998) 438–444.